Sustainable Food Technology

ROYAL SOCIETY OF CHEMISTRY

PAPER

View Article Online
View Journal



Cite this: DOI: 10.1039/d5fb00694e

# Role of phosphorylated corn starch in the texturization of high moisture meat analogues

R. Arjun,[ab] R. Keerthi,[b] P. Monica[b] and K. V. Ragavan *[bc]

Native corn starch (NCS) is a versatile ingredient in the formulation of a wide range of extruded food products. Its low heat endurance, intolerance to low temperatures, anti-shearing properties and tendency to retrograde limit its application in production of high moisture extrudates, despite its good texturization potential. Cross-linking of corn starch by phosphorylation can improve thermal stability during high moisture extrusion. To the best of our knowledge this is the first study reporting the application of phosphorylated corn starch in high moisture extrudates. The corn starch was phosphorylated using phosphorus oxychloride ($POCl_3$) with concentrations of 0.01%, 0.04%, 0.1%, and 0.3%. The phosphate content of the PCS was found to be 0.16% and 0.31% for 0.01% and 0.04% $POCl_3$, respectively. Corn starch phosphorylated using 0.3% $POCl_3$ exhibited 34.82% higher Water Solubility Index (WSI) and 363.44% lower swelling power than native corn starch (NCS). Phosphorylated corn starches exhibited A-type crystallinity similar to native corn starch (cI 52.8%; $T_p$ 88 °C) but with decreased crystallinity indices (cI: 41.52–47.06%) and low gelatinization temperature ($T_p$: 68–80 °C). PCS was utilised in high moisture extrusion of meat analogues (HMMAs). High moisture meat analogues containing PCS resulted in a highly fibrous anisotropic structure compared to extrudates containing the native corn starch. Extrudates containing soy protein isolate (SPI) and phosphorylated corn starch (0.04% $POCl_3$) showcased a marginal increase (0.04%) in expansion ratio (ER), a 0.09% increase in bulk density, a 0.02% increase in oil absorption index (OAI) and a marginal decrease of 0.27% in degree of starch gelatinization (DSG), and a significant increase of 21.5% in water absorption index (WAI) when compared with the extrudate (SPI–NCS) prepared using SPI and NCS. Findings from this study indicate that phosphorylated starch is a potential and appropriate alternative to native starches for creating HMMAs with an enhanced fibrous anisotropic structure and improved techno-functional properties.

Received 17th October 2025
Accepted 26th November 2025

DOI: 10.1039/d5fb00694e

rsc.li/susfoodtech



### Sustainability spotlight

Rising global protein demand stresses land, water and agricultural resources. It is directly linked to carbon emissions, climate change and other pressing issues pertaining to the environment and health. One of the appropriate solutions is consumption of plant-based alternative products for animal derived food products especially meat to mitigate the above issue. This study demonstrates that phosphorylation of corn starch produces a functional, food-grade structuring agent (phosphorylated corn starch – PCS) that enhances fibre formation in high-moisture meat analogues while lowering gelatinisation temperatures and enabling replacement of costly/high-purity proteins or synthetic hydrocolloids. PCS presents a viable and alternative option for animal and plant proteins in structuring anisotropic meat structures from locally available crops. The work aligns with the UN SDGs: Zero Hunger (SDG 2), Responsible Consumption and Production (SDG 12), Climate Action (SDG 13) and Industry, Innovation and Infrastructure (SDG 9).

## 1 Introduction

The global population of humans is expected to reach approximately 10.3 billion by 2084,[1] which will increase the strain on food systems to meet the growing nutritional demand, especially for proteins. Proteins, made up of amino acids, are vital for muscle growth, immune system health, and various bodily functions. Since the body cannot produce all amino acids, it is essential to obtain them through diet.[2] Currently, animal-based proteins are the primary source of protein,[3] and they are scrutinised for their significant environmental and climate effects, as well as the pollution of water bodies caused by intensive agricultural practices primarily aimed at livestock farming.[4] Food production contributes to 35% of global greenhouse gas emissions, while nearly 60% of these emissions are attributed to the use of animals for food and livestock feed.[5] No matter what method is used or how well animal food

[a]Department of Biotechnology, Government Arts College, Thiruvananthapuram, 695014, India

[b]Agro and Food Processing Technology Division, CSIR- National Institute for Interdisciplinary Science and Technology, Thiruvananthapuram, 695019, India. E-mail: kvragavan@niist.res.in; Tel: +91 471 2515 443

[c]Academy of Scientific and Innovative Research (AcSIR), Ghaziabad, 201002, India

production works, the amount of greenhouse gases, water, and land used to grow fruits, vegetables, legumes, pulses, dry grains, and other plant-based foods is usually higher than the amount of meat produced.[6] The same area of farmland that produces a specific quantity of meat and by-products could be more effectively used to generate up to 10 times more plant protein, a variation that could potentially nourish 10 to 20 times more individuals.[7] Plant-based diets could help reduce global warming by as much as one-fifth of what is needed to keep temperatures below 2 °C.[8] Thus, they have a less significant impact on the environment than diets high in animal meat.[9] The growing number of vegans in contemporary society has significantly contributed to the need for accelerated research on plant-based alternatives to animal products.[10]

Plant-based animal product alternatives that mimic the whole-muscle cut of animal meat are produced by various processing techniques such as extrusion, shear, spinning, and cross-linking.[11] High moisture extrusion cooking (HMEC) has been identified as the primary reconstructing approach to mimic conventional whole-muscle cuts and form more anisotropic fibrous structures from plant proteins. Plant proteins may aggregate into particles and form anisotropic fibrils *via* physicochemical interactions, imparting meat-like texture and mouthfeel.[12] In most plant-based meat alternatives, polysaccharides and protein isolates are used for the development of nutritional and functionally beneficial products. Soy protein isolate (SPI) is the most frequently used protein source, but other protein sources, such as isolates from peas, lentils, lupine, chickpeas, fava beans, and mung beans, are also utilised. Additionally, protein sources derived from oilseeds, such as rapeseed and sunflower seeds, are also being used.[13] In addition to protein sources, starches are also used in plant-based meat analogues. Throughout the past few decades, extensive research has been conducted on the use of starches in meat products. It acts as a filler in meat products made from minced meat, such as sausages and beef patties.[14,15] Acquiring protein isolates such as pea or mung bean can be expensive and challenging in areas where they are not readily accessible. A viable alternative is to utilise locally available soy protein and corn starch to produce cost-effective HMMAs. This method promotes the effective formation of fibers that mimic chicken muscle.[16] The HMMAs are subjected to freeze–thaw cycles during storage and use, which can affect the internal fibrous structures. To preserve them, additives may be added to maintain the fibrous structure. Binders and other additives assist in protecting the structure and preventing texture degeneration.[13] The problem with most formulations is heat-induced gelatinisation of the starch and/or denaturation of the protein. Creating a network with the starch gels is not efficient for a better degree of fiber formation.[17,18] Native starches are widely used as a gelling agent, thickener and stabiliser in the food industry.[19] However, native starch has limited functionality, which hinders its application. Its conservative structure limits its physicochemical properties, such as thermal decomposition, high retrogradation tendency, low shear and thermal stability, and low water absorption capacity and swelling power resistance.[20]

The functionality of starch can be altered by physical, chemical and enzymatic modifications, which stabilise the starch granules during processing.[21,22] These modification approaches provide an opportunity to utilise starch as a multifunctional ingredient for the food system. Chemical modification of starches is achieved by adding a functional group or eliminating components from the starch structure.[23] The presence of three hydroxyl groups at carbon $C_2$, $C_3$, and $C_6$ in glucose makes it susceptible to substitution reactions, enabling a wide range of possible chemical modifications of starch.[24] Proper modifiers, suitable starch sources, the degree of substitution in starch, and reaction conditions (such as concentration, time, pH, and the availability of a catalyst) must be used to produce modified starches with preferred attributes and levels of substitution.[25] Cross-linking is a method that utilises several cross-linking chemicals, such as sodium trimetaphosphate (STMP), sodium tripolyphosphate (STPP), epichlorohydrin, and phosphoryl oxychloride ($POCl_3$), to chemically modify native starches.[26] The cross-linking technique (either the conventional method or reactive extrusion) influences the consistency and stability of the paste in cold storage.[27] Cross-linked starch paste reduces the amount of time starch granules break during cooking, does not thicken over time, does not break down when system acidity or shear is significantly increased, loses viscosity, and turns into a filamentous paste.[28] Phosphorylation of starch involves substitution of hydroxyl groups with phosphate groups at C-2, C-3, and C-6 positions of the glucose moieties present in amylopectin fraction. This indirectly disrupts the intramolecular H-bonding that makes up its helical crystalline structure, thereby promoting H-bonding with water molecules, resulting in increased water solubility and hydration capacity.[29] Phosphorylation results in increased hydration capacity of starch pastes after gelatinization. Because phosphate groups are extremely polar and negatively charged at physiological pH, they can create multiple hydrogen bonds and strong electrostatic interactions with water molecules, which increase hydrophilicity. Water binding capacity is also increased due to this hydrophilic nature leading to the formation of networks that enhance shear stability.[29,30] Phosphate groups also facilitate ion exchange, gel-forming and complexing activities and affect starch digestibility.[29] These factors provide the basis for chemically modifying starch by phosphorylation for industrial uses.[29,31]

Recent studies on chemical modification of starch have reported improvement of techno-functional properties. Esterification of rice bean (*Vigna umbellata*) starch has resulted in a lowering of swelling power.[32] Addition of white sorghum (*Sorghum bicolor*) starch improved its swelling power[33] Acetylated distarch adipate cassava root starch exhibited improved water binding activity and solubility.[34] Acetylation and etherification of African star apple fruit starch resulted in enhanced oil absorption capacity, swelling capacity and solubility.[35] Tapioca starch crosslinked using sodium trimetaphosphate and sodium tripolyphosphate led to better thermal stability, textural and enhanced sensory quality of soups. High-moisture extrudates containing peanut protein prepared using acetyl distarch phosphate derived from cassava starch at a concentration of 6%

improved water retention, while 12% improved emulsion activity and stability.[36] However, the application of modified corn starch with improved qualities in the production of HMMAs is yet to be explored.

In the present study, phosphorus oxychloride ($POCl_3$) was used to modify cornstarch to produce distarch phosphate (E1412). Generally, the esterification of food starch with sodium trimetaphosphate or phosphorus oxychloride is conducted according to good manufacturing practices. This process leads to cross-linking, where a polyfunctional substituent, such as phosphorus oxychloride, links two starch chains together. The structure can be illustrated as Starch–O–R–O–Starch, with R representing the cross-linking group and Starch indicating the linear and/or branched structure. Additionally, distarch phosphate may undergo treatment with acids, alkalis, enzymes, or bleaching agents in line with good manufacturing practices.[37] The phosphorylated corn starch was subjected to biochemical and morphological characterization. We also examined the effects of phosphorylated corn starch (PCS) on the structural and functional properties of HMMAs in combination with soy protein isolate (SPI). Importantly, the objective of the work is to evaluate whether chemically modified cornstarch using $POCl_3$ can be utilised in the production of HMMAs with better anisotropic fibrous structures.

# 2 Materials and methods

Corn (*Zea mays*) starch (007FGF0110123) with a purity of 83.9% was procured from Angel Starch, Erode, India. It was found to have a moisture content of 12.95% and a 3% starch solution has a viscosity of 103 cP at 80 °C and 100 rpm. Amylose and amylopectin contents were found to be 23.1% and 76.9%, respectively. Soy protein isolate was procured from Siddhi Vinayak Corporation, Indore, India. $POCl_3$, hydrochloric acid, sulphuric acid, hexane, ethanol, sodium chloride, sodium hydroxide, potassium hydroxide, potassium sulphate, copper sulphate anhydrous, potassium iodide, potassium bromide, and phenolphthalein (analytical grade) were procured from Sigma Aldrich, USA. All other chemicals were of analytical grade, and double-distilled water was used for analysis throughout the study.

## 2.1 Phosphorylation of corn starch

The corn starch was phosphorylated using $POCl_3$ using a procedure with slight modification.[38] Briefly, 100 g of NCS was suspended in 150 mL of double-distilled water, and the pH of the solution was adjusted to 11 using 0.1 M NaOH. After adding 0.1% NaCl based on the dry weight of starch, $POCl_3$ (0.01%, 0.04%, 0.1%, and 0.3%) was added and slowly stirred into the respective solutions at room temperature. The mixture was stirred for 1.5 h, and the $POCl_3$ starch reaction was stopped by acidifying it with a 2% solution of concentrated HCl to achieve a pH of 5. The mixture was filtered and washed twice in 200 mL of double-distilled water and then dried for 24 h at 50 °C in a hot air oven.

## 2.2 Characterisation of starches

**2.2.1 Estimation of phosphate content.** The phosphate content of the phosphorylated starch was estimated with a modified[39] titrimetric method.[40] Briefly, 1 g of phosphorylated corn starch was mixed with 50 mL of 75% ethanol and stirred at 170 rpm for 30 min at 50 °C. After cooling the mixture to room temperature, 40 mL of 0.5 M KOH was added and stirred for 24 h to achieve a homogeneous solution. The surplus alkali was titrated with 5.0 M HCl using phenolphthalein as an indicator. The NCS solution was used as a blank solution in the assay. The phosphate content was calculated using eqn (1):

$$\text{Phosphate}(\%) = \frac{[(\text{blank} - \text{sample}) \times \text{molarity of HCl} \times 0.031 \times 100]}{\text{sample weight}} \quad (1)$$

**2.2.2 Degree of substitution.** The degree of substitution was determined using eqn (2),[39] and was computed as follows:

$$\text{DS} = \frac{162 \times P}{3100 - (102 \times P)} \quad (2)$$

where $P$ represents the percentage of phosphate calculated through the titrimetric method, 162 is the molecular weight of anhydroglucose, 31 is the atomic weight of phosphorus multiplied by 100, and 102 is the molar mass of the phosphate in distarch phosphate.

**2.2.3 Water solubility index and swelling power.** Water solubility index (WSI) and swelling power (SP) of the starches were calculated with slight modification of the protocols reported in the literature.[41] Briefly, 2.5 g ($W_1$) of starch was dispersed in 30 mL of double-distilled water, transferred to a 50 mL pre-weighed centrifuge tube, and placed at 80 °C in a water bath for 30 minutes with constant stirring. The solution was cooled to room temperature, then centrifuged at 3000 rpm for 10 min to separate the supernatant and dried at 105 °C for 1 h. The weight of the dried supernatant was calculated and noted as $W_2$. The weight of the pellet/sediment was assigned as $W_3$. The SP and WSI of the starch were calculated using eqn (3) and (4).

$$\text{Water solubility index}(\text{WSI}\%) = \left(\frac{\text{weight of dried supernatant } (W_2)}{\text{weight of original sample}(W_1)}\right) \times 100 \quad (3)$$

$$\text{Swelling power}(\text{SP}\%) = \left(\frac{\text{weight of sediment}(W_3)}{\text{weight of original sample}(W_1)}\right) \times 100 \quad (4)$$

**2.2.4 Starch paste clarity.** The paste clarity of NCS and PCS was determined based on the following method.[42] Briefly, a 1% starch solution was prepared with double-distilled water, heated to 95 °C for an hour with constant stirring, and then cooled to room temperature. Absorbance of the solution was

measured at 650 nm using a spectrophotometer (SHIMADZU 1801, Japan). Transmittance and turbidity of the starch solution were determined using eqn (5) and (6).

$$\text{Transmittance (\%)} = \text{antilog}\,(2 - \text{absorbance}) \quad (5)$$

$$\text{Turbidity (\%)} = (100 - \%\ \text{transmittance}) \quad (6)$$

**2.2.5 Differential scanning calorimetry.** The Differential Scanning Calorimetry (DSC) curves of NCS and PCSs were recorded using a differential scanning calorimeter (Mettler Toledo DSC821e, Columbus, Ohio, USA) with a heating rate of 10 °C $min^{-1}$ in the range of 30 to 130 °C. Approximately 3 mg of sample was taken with twice the amount of distilled water in an aluminium DSC pan and allowed to equilibrate overnight at room temperature. The respective thermograms were recorded using an empty aluminium pan as a reference. From the thermograms, thermal transitions of starch were interpreted and described in terms of temperature at $T_o$ (onset), $T_p$ (peak), and $T_c$ (completion). The fluctuation in crystalline stability is reflected in the value of $T_c - T_o$, and $\Delta H$ depicts the enthalpy of transition (J $g^{-1}$).

**2.2.6 X-ray diffraction.** The crystalline and amorphous nature of NCS and PCS was analysed using an X-ray diffractometer (XRD) (Malvern analytical Empyrean 3 diffractometer, UK and Almelo, Netherlands) with a Ni-filtered Cu-Kα ($\lambda = 1.54$ Å) beam of 45 kV and 30 mA. Samples were scanned in the range of 10–90°, with a speed of 1°/min. Crystallinity index of the samples was calculated using eqn (7) in Origin (pro) (version 8.5, OriginLab Corporation, Northampton, MA, USA).

$$\text{Crystallinity index}(\%) = \left(\frac{\text{sum of crystalline peak areas}}{\text{sum of crystalline and amorphous peak areas}}\right) \times 100 \quad (7)$$

**2.2.7 Fourier transform infrared spectroscopy.** The Fourier transform infrared (FTIR) spectra of NCS and PCSs were recorded using an FTIR spectrophotometer (Bruker Alpha-T, Germany) in the region from 400–4000 $cm^{-1}$. The starch samples were pressed into pellets with KBr.

**2.2.8 Scanning electron microscopy.** Morphology of the NCS and PCS samples was investigated using a scanning electron microscope (SEM) (SEM, Zeiss EVO 18 Cryo SEM, Jena, Germany), operated at an accelerating voltage of 15 kV. Samples were sputter-coated and analysed at 3 distinct magnifications, *viz.*, 2.50 KX, 3.00 KX, and 3.50 KX.

### 2.3 High moisture extrusion

High moisture extrudates are obtained through a lab-scale twin screw extruder (Basic Technologies Private Ltd, Kolkata, India) attached to an indigenously designed cooling die having three distinct temperature zones (19 °C, 15 °C, and 11 °C). Extrusion feed containing 60% moisture and 40% solids (80% of SPI and 20% of NCS/PCS) was extruded at a maximum barrel temperature of 120 °C, a screw speed of 350 rpm, and a torque of 4 Nm. Extruded samples were placed inside polythene zip-lock bags and stored at 4 °C till further analysis.

### 2.4 Quality evaluation of high moisture meat analogues (HMMAs)

**2.4.1 Proximate analysis of starches and HMMAs.** Nutritional composition of the starches and the HMMA was analysed according to the AOAC Official Method.[43–47]

**2.4.2 Expansion ratio (ER).** Expansion ratio (ER) of the HMMA was calculated with slight modification using eqn (8).[48]

$$\text{Expansion ratio} = \frac{b^2}{b_{die}{}^2} \quad (8)$$

Here, $b$ is the average breadth of the extrudate, and $b_{die}$ represents the breadth of the die.

**2.4.3 Bulk density.** The HMMA samples were weighed and filled into a cylindrical container with a predetermined volume of 1000 mL. Measurements were carried out in triplicate, and the average was taken. The equation given below (eqn (9)) was used to find the extrudate's bulk density.[49]

$$\text{Bulk density}\left(\text{g cm}^3\right) = \frac{W_1}{V_c} \quad (9)$$

where $V_c$ is the volume of the cylindrical container (1000 mL) and $W_1$ is the extrudate weight (g) taken.

**2.4.4 Water absorption and oil absorption indices.** Water absorption index (WAI) of the HMMA was calculated using the centrifuge method with slight modification.[48] Briefly, 2 g of HMMA were put into a centrifuge tube with 25 mL of distilled water, and kept for 30 min at 30 °C in a water bath, and the suspension was centrifuged at 3700 rpm for 15 min. After removing the supernatant, the weight of the precipitate was measured, and WAI was calculated using eqn (10) given below .

$$\text{WAI} = \frac{W_2}{W_0} \times 100\% \quad (10)$$

where $W_0$ is the dried sample weight and $W_2$ is the precipitate weight (g).

Oil absorption index (OAI) of the HMMA was also calculated using the same centrifuge method[50] with slight modification. Instead of water, 25 mL of oil was used, and OAI was calculated using eqn (11):

$$\text{OAI} = \frac{W_2}{W_0} \times 100\% \quad (11)$$

where $W_0$ is the dried sample weight and $W_2$ is the precipitate weight (g).

**2.4.5 Evaluation of colour.** The colour analysis of the HMMA was performed by using a Hunter Lab Colorimeter, (Colour Flex EZ, CFE21536, Virginia, USA). Measured values were expressed in the form of $L^*$ (lightness), $a^*$ (yellowness) and $b^*$ (redness).

**2.4.6 Degree of starch gelatinization.** The degree of starch gelatinization (DSG) was calculated according to the reported protocol.[51] For the analysis, 40 mg of HMMA was dispersed in 40 mL of 0.06 N KOH and gently stirred for 20 min, and then

centrifuged at 3200 rpm for 10 min. To 1 mL of supernatant, 8 mL of distilled water was added along with 1 mL of 0.06 N HCl and 0.1 mL of 1% potassium iodide. For the control, only 0.5 N KOH, 0.5 N HCl, 8 mL of distilled water, and 0.1 mL of 1% potassium iodide were added. Absorbance of the solutions was measured at 600 nm. Measurements were done in triplicate and averaged. DSG was then calculated using eqn (12)

$$\mathrm{DSG} = \frac{A_1}{A_2} \tag{12}$$

where $A_1$ is the sample group's absorbance at 600 nm and $A_2$ is the control group's absorbance.

# 3 Results and discussion

## 3.1 Phosphorylation of corn starch

Starch phosphates are prepared through an esterification reaction with the following reactants: ortho-phosphoric acid, sodium or potassium ortho-phosphate, and sodium tripolyphosphate, to obtain mono-starch phosphates. In contrast, STMP or phosphorus oxychloride ($POCl_3$) is used as a reactant to obtain distarch phosphates. The phosphorylation of corn starch was performed using phosphorus oxychloride ($POCl_3$) at different concentrations of 0.01%, 0.04%, 0.1%, and 0.3% (w/w, based on the dry weight of the starch). These concentrations were chosen to optimise the level of phosphorylation while adhering to regulatory limits. The process of preparing distarch phosphates restricts the use of sodium trimetaphosphate to a maximum concentration of 1% or allows for up to 0.1% phosphorus oxychloride.[52] Therefore, the selected $POCl_3$ concentrations were intended to achieve efficient starch crosslinking without exceeding the allowable residual phosphate levels. The phosphate content in the phosphorylated corn starch (PCS) samples was then measured calorimetrically using the specified method (Fig. 1a). $POCl_3$ reacts rapidly with starch, leading to the formation of di-starch phosphate, a crosslinked starch structure.[53] Upon introduction into the aqueous starch system, $POCl_3$ undergoes hydrolysis. The first chloride ion is displaced within a very short half-life of 0.01 s, forming phosphoryl dichloride ($POCl_2$), the primary reactive intermediate responsible for starch crosslinking.[54] This phosphoryl dichloride intermediate has a longer lifetime of approximately 4 min and further hydrolyses in the presence of water, displacing the remaining chloride ions. For efficient crosslinking to occur, $POCl_3$ must interact with starch granules before complete hydrolysis, allowing the *in situ* generated phosphoryl intermediates to react with hydroxyl groups on the starch, thereby forming phosphate bridges between starch chains.[55,56]

## 3.2 Characterization of phosphorylated corn starch

**3.2.1 Phosphate content.** The extent of phosphorylation of corn starch by $POCl_3$ was measured and found to increase with increasing concentration of the reactant. It ranged from 0.16 to 0.93% for a reactant concentration of 0.01 to 0.3% (Fig. 1a). According to Commission Regulation (EU) No. 231/2012 and JECFA 2016a, the maximum permitted phosphate content in terms of phosphorus is 0.5% for wheat and potato starches, while for starches from other sources, including corn, it is 0.4%.[57] It was evident from the table that $POCl_3$ concentrations of 0.01% and 0.04% resulted in phosphate contents of 0.16% and 0.31% in the final product, which were below the prescribed regulatory limits for di-starch phosphate. The phosphorylation of sago starch with 4% $POCl_3$ at different pH levels (8, 9, 10, and 11) produced distarch phosphate with phosphate levels of 0.02%, 0.28%, 0.29%, and 0.35%, respectively. This increase in pH from 8 to 11 resulted in a total phosphorus content rise of over 100% in the final product.[58] This trend aligns with previous research suggesting that the substitution predominantly occurs at the hydroxyl groups on the C6 position of the anhydroglucose units.[59] Additionally, the reactivity of these C6 hydroxyl groups is affected by the alkalinity of the reaction environment.[60] In the current experimental setup, phosphorylated corn starch can be synthesised using much lower concentrations of $POCl_3$ (0.01–0.04%) at pH 11 while ensuring that the phosphate content remains under the regulatory limit of 0.4%.

**3.2.2 Degree of substitution.** The degree of substitution (DS) is the average number of functional groups conjugated per

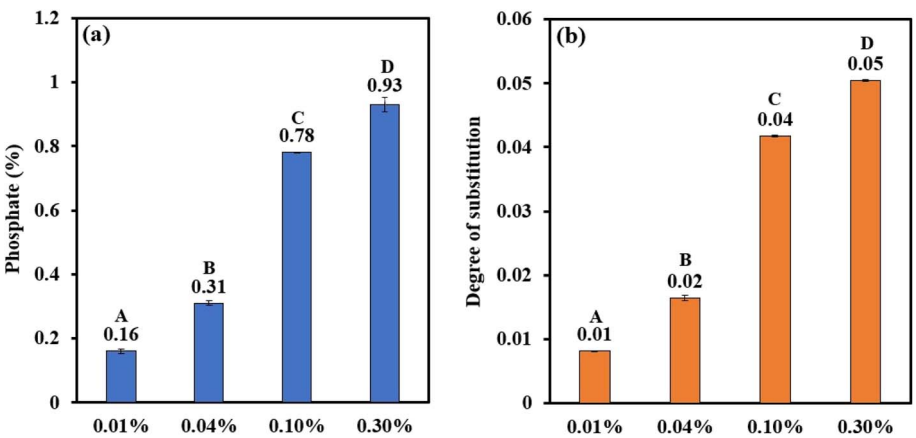


Fig. 1 Bar graph representing (a) phosphate (%) and (b) degree of substitution of PCSs. The uppercase letters (A to D) represent the significant differences ($P \leq 0.05$) among phosphate (%) and degree of substitution values analysed by the *post hoc* Tukey HSD test.

glucose unit in the starch. The DS of the phosphorylated corn starch is represented in Fig. 1b. It is evident that, with increasing concentration of $POCl_3$, the DS of the PCS was increasing with a maximum DS of 0.05 for 0.3% $POCl_3$. The degree of substitution (DS) for phosphorylated sago starch prepared with $POCl_3$ tended to increase as the pH level rose from 8 to 11. The findings verify that the DS was influenced by the pH of the reaction mixture.[61] This outcome was anticipated since a higher pH promotes starch phosphorylation.[62] The rise in DS could be attributed to the enhanced reactivity of OH groups at C6, which depended on the alkalinity of the reaction mixture.[60] The presence of sodium ions in the reaction media is also reported to contribute to the reaction kinetics.[63]

**3.2.3 Water solubility index and swelling power.** Water solubility index (WSI) and swelling power (SP) are two critical parameters controlling the techno-functional and sensory attributes of HMMAs. WSI and SP of the NCS and PCS were evaluated to formulate the feed for high moisture extrusion (Fig. 2). The water solubility index (WSI) exhibited a slight increase following the phosphorylation of native corn starch (NCS), except for the sample treated with 0.3% $POCl_3$, which showed a notable rise in WSI. NCS recorded the lowest WSI at 3.56%, whereas the phosphorylated corn starch (PCS) treated with 0.3% $POCl_3$ achieved the highest value of 38.38%. This pattern contrasts with earlier studies, which indicated that the WSI of phosphorylated sago starch was lower than that of its native form.[58] The difference could be due to variations in the starch source, the type of phosphate reagent used, and the structural changes that occur during the esterification process.

In case of swelling power, a different trend was observed for the phosphorylated corn starch compared to WSI. NCS had the highest swelling power of 882.9%, which gradually decreased with phosphorylation and PCS with 0.3% $POCl_3$ had the lowest value of 519.46%. It is evident that phosphorylation decreased the swelling capacity of corn starch, and the trend is consistent with the reported literature.[64] In the above study, the swelling power of cross-linked oat starch was found to be inversely proportional to the extent of cross-linking. It is well known that cross-linking restricts the dynamic movement of starch chains, enabling them to resist swelling. The development of intermolecular bridges by phosphorus residue following the cross-linking reaction would, in turn, explain the lower swelling factor.[26] It is expected that lower swelling power might assist in retaining the anisotropic fibrous structure of the high moisture extrudates.

**3.2.4 Percentage of transmittance and turbidity.** There is a clear correlation between starch gelation and turbidity, a measurement of light scattering in a liquid. Amylose molecules leach out, as starch granules swell and decompose during the gelatinization process, creating networks resulting in increased turbidity. The size of starch granules, swelling, granule remains, and the molecular weight of amylose and amylopectin are all factors that affect turbidity.[65] The percentage of transmittance and turbidity of native and phosphorylated corn starches were obtained spectrophotometrically, and are given in Fig. 3: (a) percentage of transmittance and (b) turbidity. The light transmittance values of the starches were in the range of 42.34% to 59.43%, with NCS having the lowest and PCS (0.04% $POCl_3$) having the highest values. Only PCS (0.01% $POCl_3$) had a lower transmittance, 42.34%, than NCS. In turn, PCS (0.01% $POCl_3$) had the highest turbidity of 57.7%. The conditions of the starch suspension during dispersion and the starch propensity for retrogradation directly affect paste clarity.[58] According to Yang *et al.*,[66] 2016 and Zheng *et al.*,[67] 2017, the negatively charged phosphate groups' attraction to neighboring starch molecules appeared to minimise inter-chain connections while increasing the number of hydrated molecules and, consequently, the paste clarity. A poor transmittance indicates that the majority of light entering the sample is scattered by coacervate droplets or other particles suspended in the sample.[42] Such samples will show a clear hazy appearance. The phosphorylated corn starches (PCSs) developed in this study displayed greater transmittance and reduced turbidity in comparison to native corn starch (NCS), except the PCS treated with 0.01% $POCl_3$. When applied in the production of high-moisture meat analogues (HMMAs), these PCSs – due to their superior gelatinization characteristics – facilitated the creation of a more distinct anisotropic fibrous structure relative to HMMAs made with NCS or other PCS variants.

**3.2.5 DSC.** Starch undergoes a unique sequence of events at the molecular level when heated with water, bringing in drastic changes in its rheological properties. It is essential to

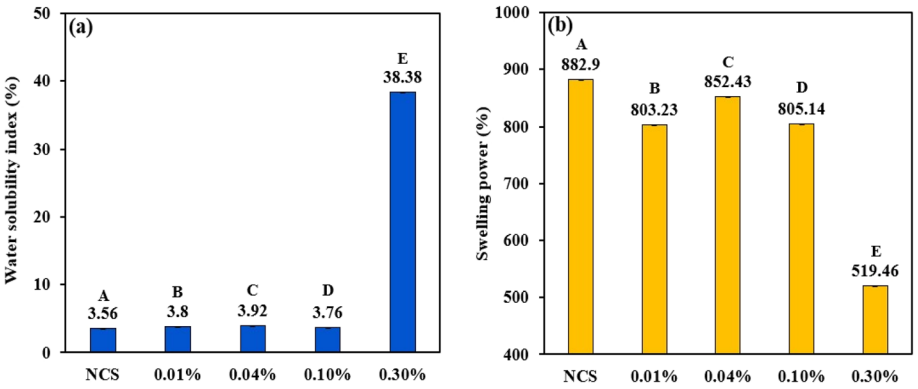


Fig. 2 Bar graph representing (a) WSI and (b) SP of NCS and PCSs. The uppercase letters (A to E) represent the significant differences ($P \leq 0.05$) among WSI and swelling power values analysed by the *post hoc* Tukey HSD test.

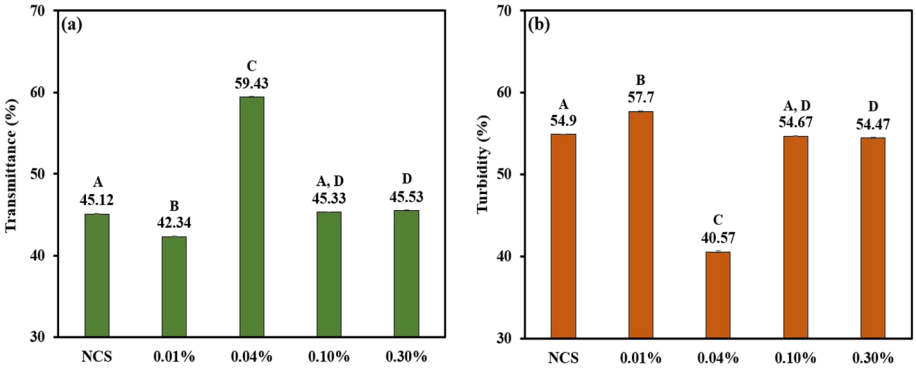


Fig. 3 Bar graph representing (a) transmittance and (b) turbidity of NCS and PCSs. The uppercase letters (A to D) represent the significant differences ($P \leq 0.05$) among transmittance and turbidity values analysed by the *post hoc* Tukey HSD test.

understand the role of starch during the high moisture extrusion process to optimise the process to control the fibrous structure of the extrudates.[68] Phosphorylation induces changes in the starch structure, and the newly introduced phosphate group is expected to impact its gelatinisation behaviour, which is analysed through DSC, and it was found to exhibit significant changes in the DSC thermograms (Fig. 4 & Table 1). The gelatinisation temperature ($T_p$) of NCS was found to be 88 °C, whereas the gelatinization temperature ($T_p$) of the modified starches was found to be lower in the range 68–80 °C. This indicates that the modified starches are easily gelatinized than the native starch. It was also observed that with an increase in phosphorylation content, the gelatinization parameters ($T_0$, $T_p$ and $T_c$) of corn starch were decreasing. Phosphorylation of starch involves substitution of –OH groups at the C-2, C-3, and C-6 positions of the glucose moieties present in the amylopectin fraction of corn starch.[29] This indirectly disrupts the starch structure and crystal stability by obstructing the intramolecular hydrogen bond formation required for the establishment of double helices.[69] The destabilization of starch structures brought about by steric hindrance and repulsive force from newly introduced negatively charged phosphate groups alters the starch granule morphology and causes relatively easy uncoiling of amylopectin double helices.[66,67] It leads to an amorphous starch structure, which requires less energy for gelatinization (enthalpy of gelatinization – $\Delta H$)[70,71] and plasticization. Expanded structures of starch will have higher randomness and increased possibilities for intramolecular hydrogen bonding and network formation. Moreover, the reduction in gelatinization temperature was found to correlate with the reduction in overall crystallinity index of the phosphorylated corn starch analysed through XRD (discussed in the next section). Similar trends in gelatinization parameters were reported during phosphorylation of chestnut[70,72] and waxy rice starch.[73] Degree of substitution and granule rigidity are other factors that affect the thermal properties.[72] Low enthalpy and gelatinization temperature reduce energy consumption and production cost during food processing.[66] Overall, phosphorylation of NCS is expected to have lower and mild extrusion conditions for the production of HMMAs.

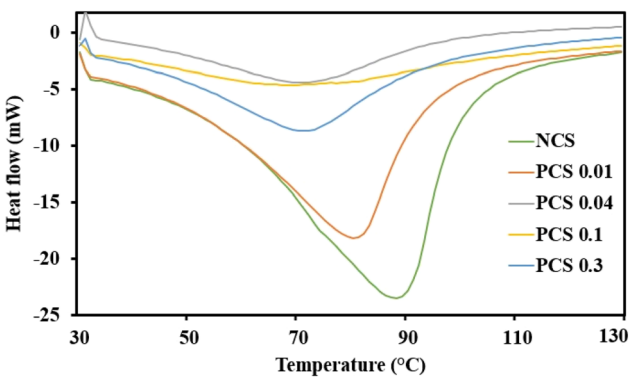


Fig. 4 Differential scanning calorimetry (DSC) curves of NCS and PCSs.

**3.2.6 XRD.** It is a well-known phenomenon that changes in the native starch structure and composition inherently impact its crystalline integrity with an increase in amorphous regions. To understand the role of phosphorylation in the crystalline structure of native corn starch, X-ray diffraction studies were carried out. Both the native and the phosphorylated starches exhibited characteristic A-type crystalline peaks at 15°, 17°, 18° and 23°.[74,75] The XRD pattern of modified starches indicated that phosphorylation did not affect the characteristic pattern of corn starch (A-type). However, the intensities of some of the diffraction peaks of phosphorylated corn starch were found to be reduced when compared to those of native corn starch (Fig. 5). This could be attributed to the substitution of hydroxyl groups with phosphate groups during modification of the crystalline and amorphous regions.[72] This reduction in peak intensities further led to a decrease in the crystallinity index of phosphorylated corn starch (41.52–47.06%) when compared

Table 1 DSC analysis containing gelatinization temperature ($T_p$), initial temperature ($T_0$), final temperature ($T_f$), and enthalpy of gelatinization ($\Delta H$) of NCS and PCSs

| Starch | $T_p$ (°C) | $T_0$ (°C) | $T_f$ (°C) | $\Delta H$ (J g$^{-1}$) |
|---|---|---|---|---|
| NCS | 88 | 34 | 106 | 88.97 |
| PCS 0.01 | 80 | 36 | 95 | 76.87 |
| PCS 0.04 | 71 | 37 | 97 | 77.99 |
| PCS 0.1 | 68 | 33 | 112.25 | 94.63 |
| PCS 0.3 | 71 | 35 | 94 | 70.74 |

with native corn starch (52.8%). Phosphorylation decreased the crystallinity of the starch granule without affecting its A-type structure.[66] It might have reduced the intra/inter-molecular hydrogen bond formation, thereby disrupting the helical crystalline structure of the starch granules.[72] The stability of starch granules is directly proportional to their gelatinization enthalpy.[76] A decrease in crystallinity and thermal stability reduces the energy needed for starch gelatinization during high-moisture extrusion, which improves its meltability, aids in chain alignment, and encourages more effective fiber formation in meat alternatives. This interpretation is supported by the reduction in gelatinization enthalpy ($\Delta H$) that was observed with an increase in degree of phosphorylation in the DSC analysis. A decrease in crystallinity of corn starch after phosphorylation, without affecting its A-type crystallinity, was reported.[74] This clarifies why phosphorylated starch, even though it retains its A-type structure, is more successful in creating anisotropic textures in HMMA applications.

**3.2.7 FTIR.** The impact of phosphorylation on the molecular structure of NCS and PCSs was evaluated using FT-IR analysis. FTIR spectra of NCS and PCS were almost similar, with the latter exhibiting the characteristic peaks of the phosphate group (Fig. 6a & b). Wide bands observed between 3000 and 3500 $cm^{-1}$ could be attributed to O–H stretching vibrations.[66] A weak band around 2900 $cm^{-1}$ indicates asymmetric stretching of C–H bonds. Vibrations in H–O–H bonds are denoted by a sharp peak around 1650 $cm^{-1}$.[70] This peak could also indicate absorption of water in the amorphous region of starch.[77] C–H stretching of the alkane group was indicated by the narrow bands around 1330 $cm^{-1}$ and 1370 $cm^{-1}$.[74] A narrow band around 1000 $cm^{-1}$ could be attributed to the stretching vibration of C–O bonds. Stretching vibrations of C–O–C could be attributed to bands around 1140 $cm^{-1}$. A small sharp band around 850 $cm^{-1}$ indicated D-pyran glucose.[70] The absence of bands between 1530 and 1630 $cm^{-1}$ (attributed to amide (II) bonds) indicated that the starch was pure and devoid of any protein contamination.[77] A characteristic band around 1400 $cm^{-1}$, which was observed only in the phosphorylated corn starches, can be attributed to P=O stretching vibrations.[72] The diffraction peak at 1019 $cm^{-1}$, indicating P–O–C symmetrical stretching, was not observed in any of the phosphorylated corn starch samples, which could be due to a low degree of substitution in the PCS.[70] Similar observations for the absence of bands indicating P–O–C symmetrical stretching due to a low degree of substitution in phosphorylated glutinous rice starches are reported in the literature.[66] Overall, FTIR spectra indicate the phosphorylation of NCS with low DS. Even though the level of phosphorylation is minimal, the addition of phosphate groups improves interactions between starch and water while decreasing molecular order, which is indicated by wider O–H and H–O–H absorption bands. These alterations can promote gelatinisation and increase molecular mobility during high-moisture extrusion, which facilitates better alignment and entanglement of starch chains – essential for creating fibrous, meat-like textures in HMMAs. Therefore, the FTIR findings confirm the functional effectiveness of phosphorylated corn starch in high-moisture extrusion applications, even with low degrees of substitution.

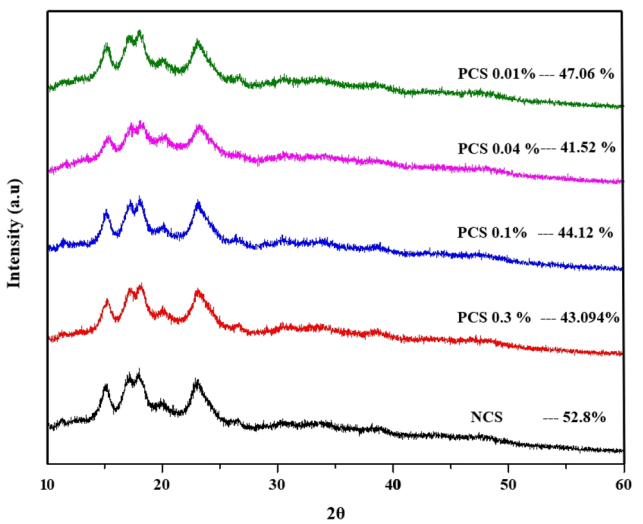


Fig. 5 X-ray diffraction patterns for NCS and PCSs and their respective crystallinity.

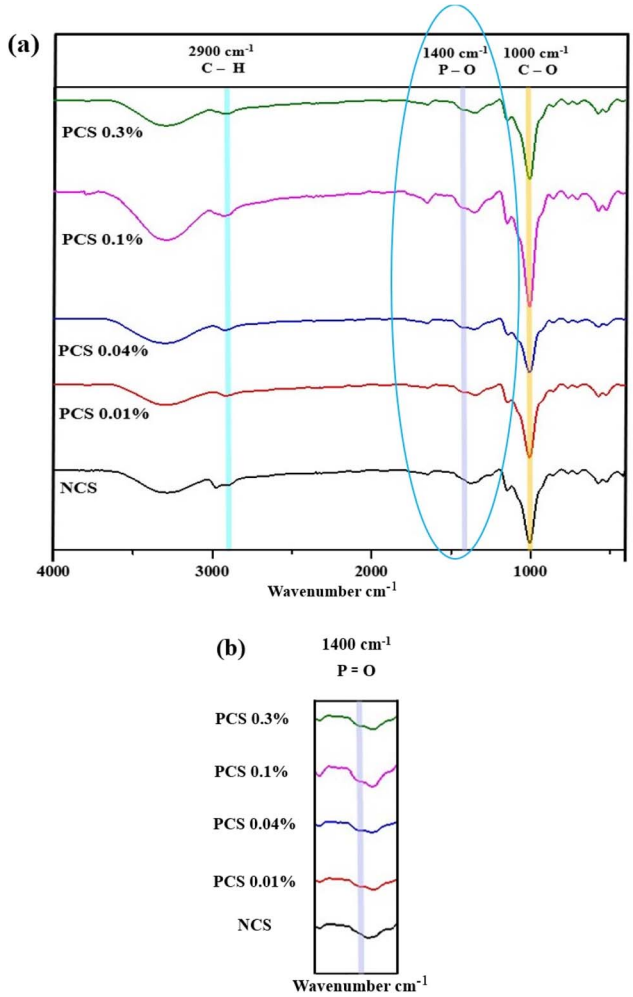


Fig. 6 (a) FTIR spectrum of starches: NCS, PCS 0.01%, PCS 0.04%, PCS 0.1% and PCS 0.3%; (b) the peak in the 1400 range, which is found only for PCSs.

**3.2.8 SEM.** The impact of phosphorylation on the morphology of starch granules was examined through SEM analysis (Fig. 7). The granule surface morphology of NCS was smooth and devoid of any pores or cracks (Fig. 7a). However, the surface morphology of the phosphorylated starch granules is found to be porous to some extent (Fig. 7b to e). Porosity in the starch granules may be attributed to the alkaline reaction conditions. Moreover, the reaction was carried out well below the gelatinization temperature, which indicates that the porosity of the starch granules is due to the phosphorylation reaction. A reactant with a very low lifetime can react only with the surface OH groups of the starch granule. Furthermore, the surface of the granules will most likely sustain damage in alkaline environments, as observed in other studies.[78] The improved surface porosity aligns with the noted rise in the water solubility index (WSI) since the altered surface of the granules facilitates a greater discharge of soluble components. The weak binding force between the crystalline and non-crystalline layers during crosslinking makes it susceptible to damage and causes minute cracks and porous structures (Fig. 7). The degree of damage and crystallization of the granules increase with increasing degree of substitution.[62] The increased porosity helps granules absorb more water. In the cooling zone, porous starch particles can serve as fillers, weaken the continuous protein phase, and result in a softer texture and less extrudate expansion.[79] These changes in morphology and hydration can be beneficial during high-moisture extrusion, as the increased solubility and partial breakdown of granules may improve starch mobility and promote cross-linking under shear, leading to the development of a fibrous texture in meat analogues.

### 3.3 High-moisture meat analogues

High moisture meat analogues (HMMAs) were extruded with an indigenous cooling die (SI, Fig. S1) with the following formulations. A feed containing 80% SPI and 20% NCS did not yield a significant fibrous structure in the extrudate. Instead, a homogeneous soft gel-like mass with a limited fibrous structure resembling strips or flaps was obtained. It confirms the

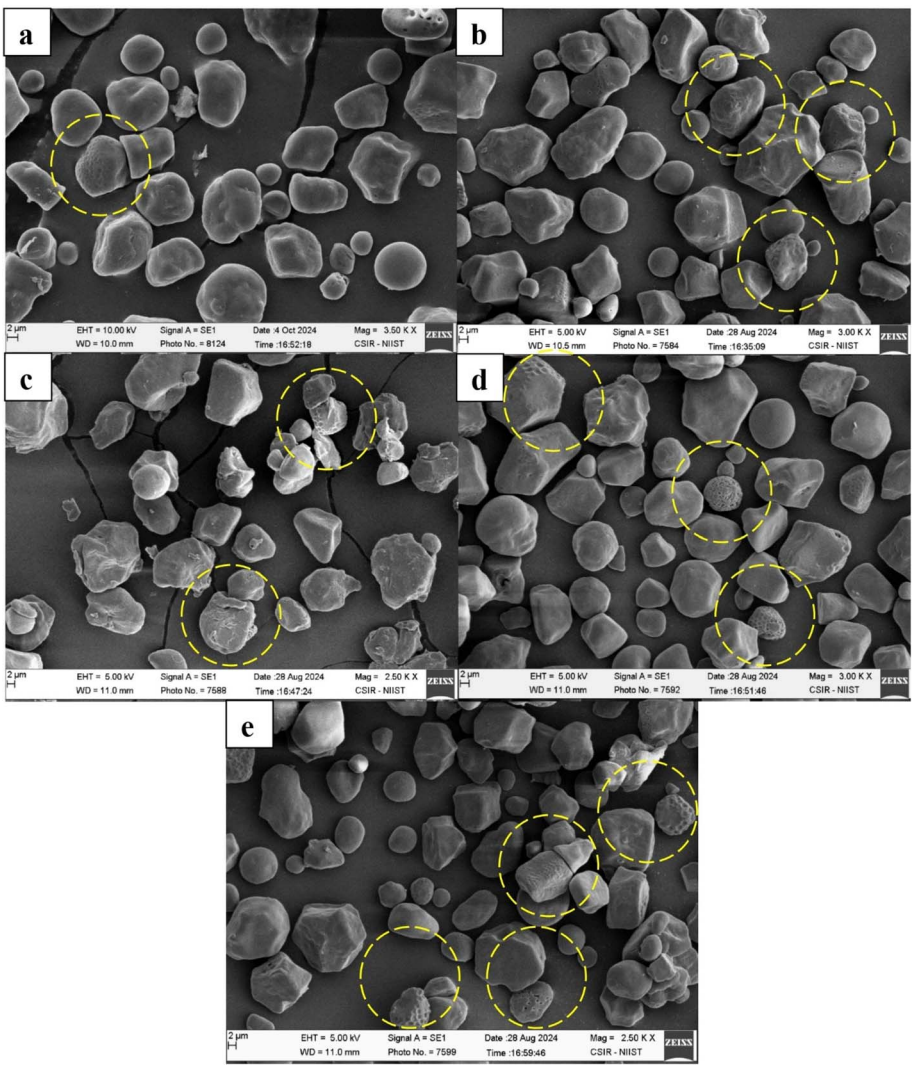


Fig. 7 SEM images of (a) NCS, (b) PCS 0.01%, (c) PCS 0.04%, (d) PCS 0.1%, and (e) PCS 0.3%. Yellow dotted circles indicate the degree of fissures on the surface of starch granules.

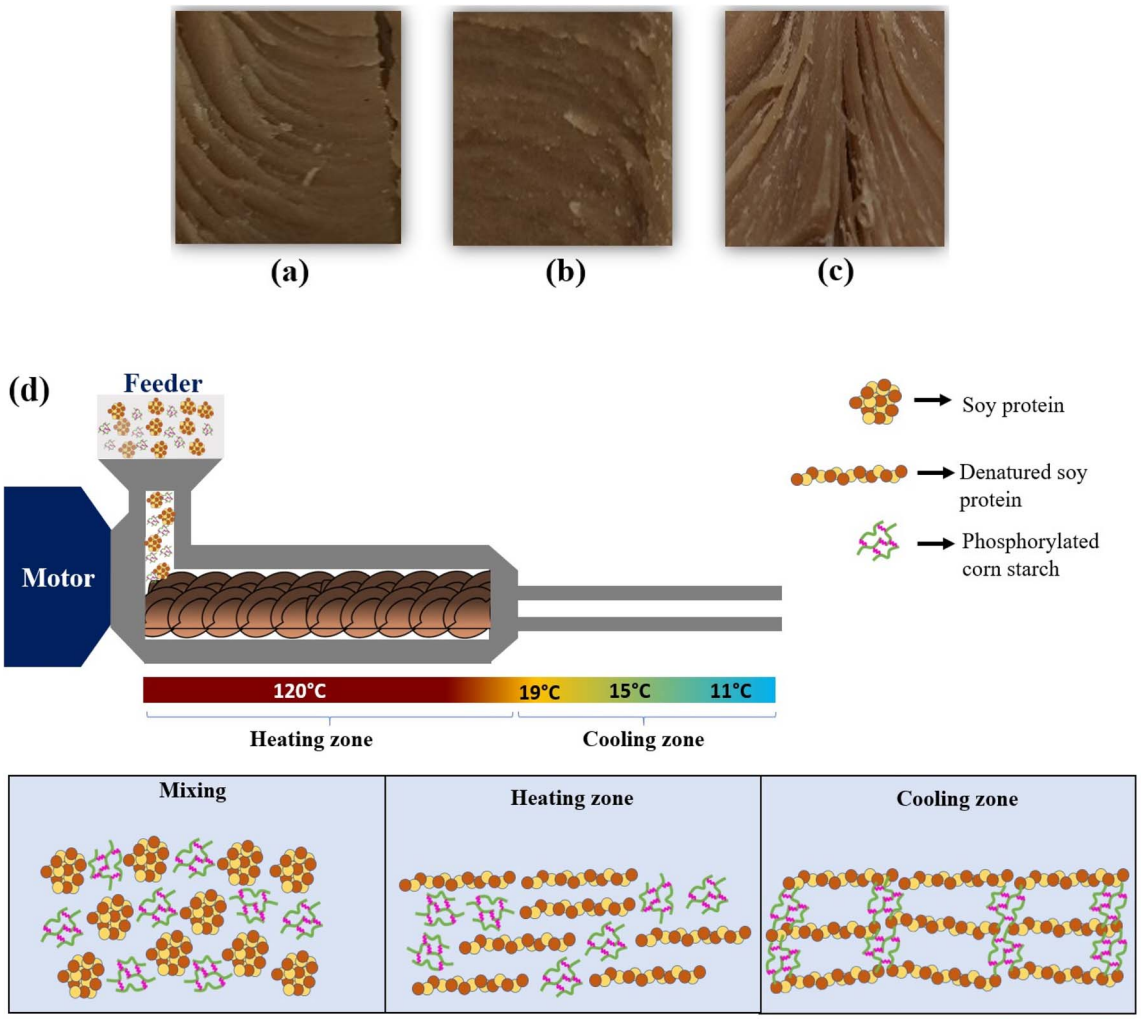


Fig. 8 (a) HMMAs from SPI–NCS (80 : 20) showing a moderate fibrous structure. (b) SPI–PCS (0.04% $POCl_3$, 80 : 20) showing less fiber formation. (c) SPI–PCS (0.01% $POCl_3$, 80 : 20) with a distinct, thin fibrous structure. (d) Schematic illustration of the hypothesised mechanism.

lack of fibre-forming functionality of native starches during the high moisture extrusion process. It is observed to interfere with the fibrous protein alignment in the extrudate (Fig. 8a). In contrast, replacing NCS with phosphorylated corn starch (PCS) resulted in an extrudate with a visibly improved fibrous structure. The presence of PCS promoted better alignment of protein and enhanced anisotropic structuring, likely due to its modified morphology and hydration behaviour. The increased water absorption index observed in PCS (Section 3.4.4) and hydrophilic nature led to the formation of a network that enhances its shear stability.[29,30] The negatively charged phosphate group of the starch might interact with charged amino acids of the SPI, while the hydrophilic nature of the phosphate group can influence the water mobility leading to better fibrous structure formation. However, increasing the degree of phosphorylation beyond a certain threshold did not proportionally improve the fibrous texture (Fig. 8b & c). The extrusion experiments distinctly demonstrate that phosphorylated porous corn starch provides superior functionality compared to native starch in maintaining or enhancing the formation of anisotropic fibrous textures in HMMAs.

### 3.4 Quality evaluation of high moisture meat analogues (HMMAs)

**3.4.1 Proximate analysis of starches and HMMAs.** The proximate composition of the NCS and PCS was evaluated to understand the changes in their nutritional composition. The majority of the parameters of the NCS and PCS showed no significant changes, except for the ash content, which was observed to increase as the $POCl_3$ concentration increased during the esterification process (Table 2).

The proximate composition of the three HMMAs extruded with SPI, NCS and two different PCSs is reported in Table 2. The moisture content of the HMMAs was found to be in the range of 49 to 56%, which is appropriate for a plant-based HMMA.[80] The HMMA with 0.01% $POCl_3$ had the highest moisture content of 55.8%. The highest fat percentage of 3.54% was observed in the HMMA with SPI–NCS. As for the protein content, the HMMA made with PCS (0.04% and 0.01% $POCl_3$) had values of 33.26% and 34.26%, respectively, which were lower than the protein content of HMMAs produced with SPI–NCS (35.76%). But the protein contents of all HMMAs produced in the study were of

Table 2 Proximate analysis of starches and HMMAs ($n = 3$)[a]

| | Moisture (%) | Fat (%) | Ash (%) | Protein (%) | Carbohydrate (%) |
|---|---|---|---|---|---|
| **Starch** | | | | | |
| NCS | 12.95 ± 0.02 | 2.11 ± 0.04 | 0.26 ± 0.02 | 0.77 ± 0.026 | 83.9 ± 0.08 |
| PCS (0.3%) $POCl_3$ | 10.24 ± 0.1 | 2.12 ± 0.17 | 0.8 ± 0.06 | 0.070 ± 0.021 | 86.13 ± 0.16 |
| PCS (0.1%) $POCl_3$ | 14.41 ± 0.19 | 2.19 ± 0.14 | 0.59 ± 0.03 | 0.713 ± 0.021 | 82.1 ± 0.17 |
| PCS (0.04%) $POCl_3$ | 9.71 ± 0.39 | 2.23 ± 0.21 | 0.49 ± 0.02 | 0.716 ± 0.015 | 86.84 ± 0.62 |
| PCS (0.01%) $POCl_3$ | 7.03 ± 0.12 | 2.27 ± 0.22 | 0.39 ± 0.04 | 0.74 ± 0.03 | 89.58 ± 0.27 |
| **HMMA** | | | | | |
| SPI–NCS | 49.92 ± 0.091 | 3.54 ± 0.008 | 2.66 ± 0.064 | 35.76 ± 0.1514 | 7.1 ± 0.152 |
| SPI–PCS with (0.04%) $POCl_3$ | 57.52 ± 0.089 | 2.85 ± 0.01 | 2.79 ± 0.095 | 33.26 ± 0.026 | 3.58 ± 0.182 |
| SPI–PCS with (0.01%) $POCl_3$ | 55.8 ± 0.109 | 2.54 ± 0.015 | 3.27 ± 0.015 | 34.62 ± 0.04 | 3.77 ± 0.077 |

[a] NCS-native corn starch and PCS-phosphorylated corn starch; data are expressed as mean ± SD.

similar values and the change may be caused due to the mixing of dry ingredients and parameters affecting the extrusion. The HMMA produced with SPI–PCS (0.04% and 0.01% $POCl_3$) had the carbohydrate contents of 3.58% and 3.77%, respectively, which were lower than the HMMA with SPI–NCS, 7.1%. From this, it is evident that phosphorylation of starch has decreased the carbohydrate content of the HMMA when the phosphorylated starch was used for extrusion, compared to the HMMA with the SPI–NCS combination. The mineral content was highest for the HMMA with SPI–PCS (0.01% $POCl_3$) at 3.27% and the least for SPI–NCS at 2.66%. The variations in composition emphasize the practical benefits of phosphorylated starch in HMMA formulations. Increased moisture and mineral content, coupled with decreased carbohydrate levels, indicate better water retention and structural characteristics, which improve juiciness, texture, and nutritional value. Additionally, PCS enhances compatibility with SPI, promoting fiber development and minimizing syneresis, thereby serving as an essential component for clean-label, protein-rich meat alternatives.

**3.4.2 Expansion ratio.** Expansion ratio (ER) is a critical parameter indicating the impact of extrusion on the extrusion feed and also to an extent on the breakdown and transformation of components present in the feed.[81] During the extrusion process, the temperature was set at 120 °C to provide sufficient heat to denature the proteins and prevent expansion of the extrudate exiting the cooling die. Expansion ratio of the extrudates containing NCS and PCS was found to be almost similar (Fig. 9a). The SPI–NCS extrudate had the lowest ER value of 0.98, and the extrudate composed of SPI–PCS with 0.01% and 0.04% $POCl_3$ had an ER of 1.0 and 1.02, respectively. The HMMA produced with a combination of SPI–PCS (0.01%) had an expansion ratio of 1. For the HMMA, which was produced with a combination of phosphorylated corn starch, with a decrease in $POCl_3$ content from 0.04 to 0.01%, the expansion ratio was found to be decreasing. The extent of the extrudate's puffing is indicated by the expansion ratio. The extruder's internal pressure is comparatively higher than the ambient pressure, which causes a sharp pressure drop when the extrudate exits the die. Consequently, voids remain in the mixture while water vaporisation takes place. Thus, the expansion ratio increases with the amount of moisture present in the combination. Additionally, the high gelation level of the materials present in the feed also increases the expansion ratio.[82] SPI would interact with the starch during the extrusion process and rebuild through interactions between the side chains of the soy protein molecules.[83] The tensile strength of the melt before the die was improved by the cross-linking processes between SPI and starch, which

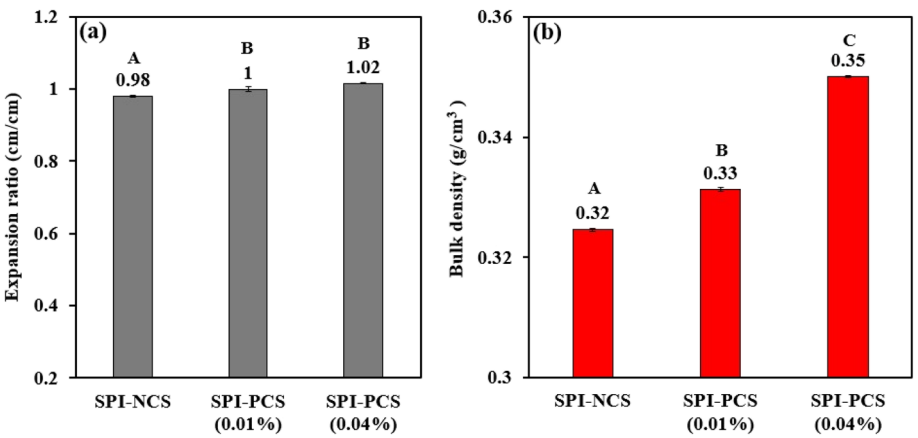


Fig. 9 Bar graph representing (a) expansion ratio and (b) bulk density of HMMAs with SPI and starch combination. The uppercase letters (A to C) represent the significant differences ($P \leq 0.05$) among expansion ratio and bulk density values analysed by the *post hoc* Tukey HSD test.

suggested that blends would experience more water flash evaporation as they depart the die.[84] Shrinkage of the extrudates after the die would be prevented by the creation of the soy protein network. It was reported that the extrudate ER increased as the processing temperature was raised from 130 to 150 °C. The materials were enlarged by the water flash after the die.[85] In this study, the temperature of the barrel was set at 120 °C for all samples, so the extrudates produced had similar expansion ratios.

**3.4.3 Bulk density.** From a business perspective, bulk density is a crucial physical characteristic of extruded items since it significantly affects their packaging needs.[86] For instance, the HMMA is lighter, its porosity is higher, and its shipping and storage costs are more detrimental when the bulk density is lower. In addition to indicating the porosity and expansion of HMMAs, changes in bulk density are linked to modifications in protein crosslinking that occur during the extrusion cooking of the feed, which is high in protein.[87] Fig. 9b shows the bulk density for the HMMA produced with SPI in combination with NCS and PCS with two different concentrations of $POCl_3$. The extrudate with NCS starch had the lowest bulk density of 0.32 g $cm^{-3}$, whereas phosphorylated corn starch, with a decrease in the concentration of $POCl_3$ from 0.04 to 0.01%, the bulk density was found to be decreasing; the extrudate with PCS (0.04% $POCl_3$) had the highest bulk density of 0.35 g $cm^{-3}$. From Fig. 10, both ER and bulk density were found to be correlated because with a decrease in $POCl_3$ concentration, ER and bulk density were found to decrease. Higher bulk density of a SPI–PCS meat analogue is linked with a denser, extra-compact structure, which improves functional properties such as texture, hardness, chewiness, and reduced product shrinkage. As per the findings of Fletcher,[88] a rise in temperature of the barrel causes the water in the extruder to become more superheated, which promotes the development of bubbles and a drop in melt viscosity, ultimately resulting in lower density, as demonstrated in this study. Extrudate density and lateral expansion have been discovered to be primarily influenced by temperature and feed moisture.[89] The observed rise in bulk density with higher screw speeds could potentially be attributed to the amplified impact of temperature on the melt of the extrudate in an elevated shear environment.[83] In our study, screw speed and barrel temperature were kept constant resulting in slight variations in bulk density between the various HMMAs produced.[90]

**3.4.4 Water absorption index and oil absorption index.** Water Absorption Index (WAI) can be defined as the amount of water bound by the starch granule after swelling under processing conditions. The thermomechanical strain during high moisture extrusion causes the starch granule to gelatinise, lose its crystalline structure and eventually break down into fragments.[91] As a result of increased surface area and exposure to water, gelation of the molecule occurs, which is quantified as WAI. In this case, WAI denotes the capacity of both the protein and starch in the extrudate. Compared to NCS, the WAI of the PCS was higher; however, an increase in the phosphorus content led to lower values (Fig. 10a). Precisely, the HMMA with NCS had a WAI of 368% and the highest WAI, 528%, was observed for the SPI–PCS with 0.01% $POCl_3$, whereas the extrudate with 0.04% $POCl_3$ had a lower WAI of 447%. There is a 43.5% increase in the WAI from SPI–NCS to SPI–PCS with 0.01% $POCl_3$ and 21.5% increase from SPI–NCS to SPI–PCS with 0.04% $POCl_3$. Starch–water, protein–water, water–water interactions, and physical capillary actions all have a significant impact on WAI.[92] WAI in nixtamalized corn flours is linked to starch crystalline structure disturbance during thermo-alkaline treatment; hence, this measure can be utilised as an indication of gelatinisation since disrupted starch granules have a greater water binding capacity. Although WSI determines the degree of polysaccharide release from water-soluble granules, high values of WAI and WSI indicate high starch granule fragmentation, dextrinization.[93,94]

A product's ability to absorb and hold oil is known as its oil absorption index (OAI), and it is recognised to enhance flavor and improve mouthfeel in food materials. The HMMA with SPI–PCS (0.04% $POCl_3$) had the highest OAI of 203.15%. The HMMA was produced by using a blend of phosphorylated corn starch and SPI; with an increase in the concentration of $POCl_3$, the OAI was found to be increasing. Fig. 10b shows OAI values for the

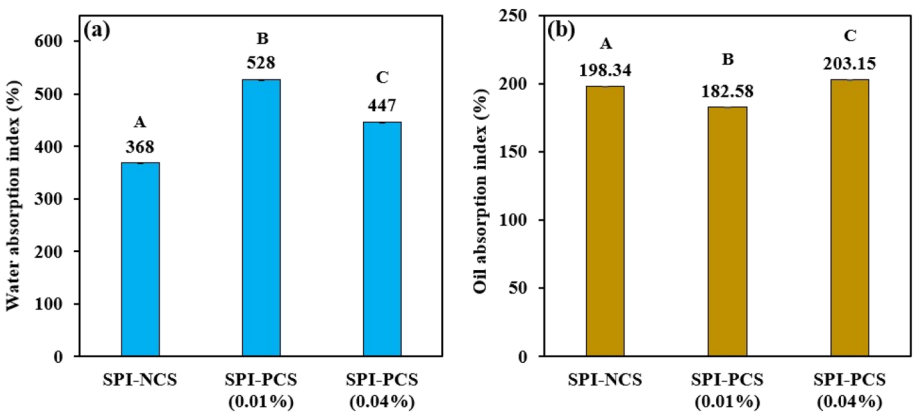


Fig. 10 Bar graph representing (a) water absorption index (WAI) and (b) oil absorption index (OAI) of the HMMA with SPI and starch combinations. The uppercase letters (A to C) represent the significant differences ($P \leq 0.05$) among WAI and OAI values analysed by the *post hoc* Tukey HSD test.

 

Table 3 Colour analysis of HMMAs ($n = 3$)[a]

| HMMA | $L^*$ | $a^*$ | $b^*$ |
|---|---|---|---|
| SPI–NCS | 44.35 ± 0.983 | 5.58 ± 0.088 | 14.19 ± 0.082 |
| SPI–PCS (0.04%) $POCl_3$ | 46.830 ± 0.262 | 7.870 ± 0.06 | 19.526 ± 0.077 |
| SPI–PCS (0.01%) $POCl_3$ | 46.890 ± 0.096 | 7.490 ± 0.02 | 19.953 ± 0.037 |

[a] NCS-native corn starch and PCS-phosphorylated corn starch; $L^*$-lightness, $a^*$-redness and $b^*$-yellowness; data are expressed as mean ± SD.

extruded HMMA produced with SPI in combination with NCS and PCS with two different concentrations of $POCl_3$. One possible explanation for the increased oil absorption could be the high degree of starch breakdown in the extrudate caused by the high heat energy input. A higher rate of oil absorption by the extrudates may be advantageous if the product is going to be used to make sauces or soups.[95] Thus, higher WAI and OAI values indicate that during cooking, when used for consumption, the meat analogue will be able to utilise the oil and water used, which will be beneficial in making various dishes and will further enhance the flavor profile of the HMMA. The results from the study indicate that product formulation can use phosphorylated starches to bring in more hydrophobic interaction in solid and liquid matrices to control the viscosity, texture and sensory aspects during food formulations.

**3.4.5 Colour analysis.** Colour of the extrudate is a critical parameter from the consumer perspective. Generally, the extrusion technique induces several processes, including the Maillard reaction, caramelization, hydrolysis, and a non-enzymatic disintegration of pigments, which leads to the colour changes in the HMMA produced.[96] Hence, it is critical to control the processing conditions to control the product quality as well as the colour of the extrudate. The colour of the extrudates containing NCS and PCS was almost the same visually. The colour values ($L^*$, $a^*$, and $b^*$) of the HMMA produced with SPI–NCS and SPI with cornstarch with 0.01% and 0.04% of $POCl_3$ are shown in Table 3. The HMMA, containing 0.01% $POCl_3$, had the highest $L^*$ (lightness) value of 46.89, whereas SPI–NCS had the lowest value of 44.35. The $a^*$ (redness) value was the lowest, 5.58 for the HMMA produced with SPI–NCS. Among HMMAs with PCS, the one with 0.01% $POCl_3$ had the lowest $a^*$ value. The HMMA with SPI–PCS (0.01% $POCl_3$) had the highest $b^*$ value of 19.95. The $b^*$ (yellowness) value of SPI–NCS was lowest when compared to other extrudates. Colour significantly influences consumer acceptance of HMMAs. The enhanced $L^*$ and $b^*$ values observed in extrudates containing phosphorylated starch suggest improved lightness and attractive yellow hues, which may result from changes in thermal and moisture interactions during the extrusion process. This suggests that PCS may regulate non-enzymatic browning reactions, leading to a more desirable and uniform appearance in meat analogues, thereby enhancing product attractiveness and marketability.

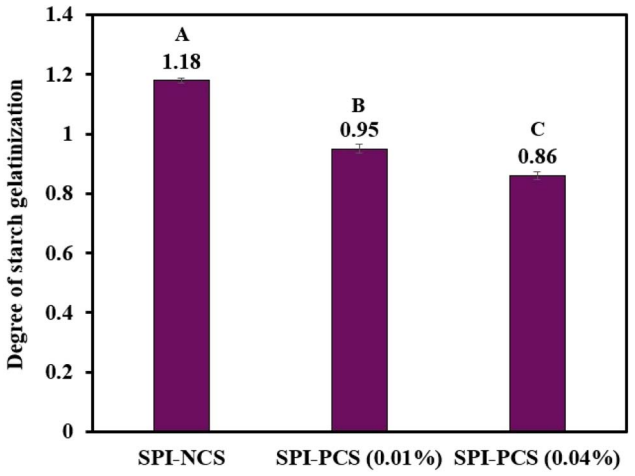


Fig. 11 Bar graph representing Degree of Starch Gelatinization (DSG) of the HMMA with SPI and starch combinations. The uppercase letters (A to C) represent the significant differences ($P \leq 0.05$) among, DSG values analysed by the *post hoc* Tukey HSD test.

**3.4.6 Degree of starch gelatinisation.** The texture, digestibility, and sensory characteristics of HMMAs are greatly influenced by the degree of starch gelatinisation (DSG). When starch granules are heated, they swell and absorb water, which causes them to lose their crystalline structure and undergo gelatinisation. The degree of this process affects the finished product's texture, ease of digestion, and even shelf life. As the DSG increases, a rise in the degree of disruption of molecules inside the granules takes place; thus, the granules' swelling and subsequent disruption change their particle size, the crystallinity and molecular weight decrease, and starch–lipid complexes are created.[97] Fig. 11 shows the DSG of the HMMA produced with SPI in combination with native corn starch and phosphorylated corn starches. The extrudate containing SPI–PCS with 0.01% $POCl_3$ had a higher DSG value of 0.95 compared to SPI–PCS with 0.04% $POCl_3$. The leached amylose and granules that remain intact after the starch has gelatinised aid in the creation of starch gels.[98] Less water is available for the starch to be gelatinised because water is distributed in the starch and the SPI matrix competitively. Due to its hydrophilic nature, phosphorylated starch binds more water and determine the aqueous phase rheology of the material.[29,79] It facilitates protein aggregation, contributing to development of the dispersed phase in the melt. The starch after gelatinization acts as a molten polymer, which then restricts protein mobility.[29,79] Phosphorylated starch increases bonding between starch (by cross-linking) and SPI as well as between the starch granules, thereby increasing viscoelasticity and extensibility.[29,79] The higher processing temperature implies that there was a greater thermal energy input into the feed inside the barrel, increasing the DSG.[90] The physicochemical characteristics of the starch, including its granule structure, gel texture, retrogradation, and heat stability, can be altered by heat and moisture treatment.[99] Therefore, in high moisture extrusion, the physicochemical attributes of the

starch used in the feed can be improved by altering the extrusion parameters such as barrel temperature, pressure, and moisture content of the feed. In this study, the temperature of the barrel was set at 120 °C for all samples, which resulted in the DSG of all the extrudates being comparable. And so, having better DSG means the starch will be able to form a better gel-matrix, which will, in turn, help in the formation of better anisotropic fibrous structures in the HMMA.

# 4 Conclusion

High-moisture extrusion cooking has proven to be one of the most effective and scalable processes for creating plant-based meat analogues, which can mimic the texture of regular animal meat while promoting environmentally sustainable and healthy living. Due to its low anti-shear properties, tendency to retrograde, ease of thermal degradation, and lack of heat endurance, the application of native starch in a variety of processed food products is restricted. In the current study, $POCl_3$ was used to produce PCS at different concentrations (0.01%, 0.04%, 0.1% and 0.3%) with varying degrees of substitution (DS). According to the EFSA Panel on Food Additives and Nutrient Sources Added to Food, the PCSs generated in this study with 0.04% $POCl_3$ and 0.01% $POCl_3$ had phosphate contents of 0.31% and 0.16%, respectively, making them suitable for addition in food products. PCS with 0.01% $POCl_3$ exhibited improved gelatinisation characteristics, evidenced by its turbidity percentage of 57.7% and its ability to withstand swelling (swelling power of ≈ 803%); therefore, it has the potential to interact with the SPI during high moisture extrusion. The HMMA formulated with PCS and SPI exhibited enhanced compactness and anisotropic fibrous structuring compared to the SPI–NCS system, with the most distinct fiber alignment observed in the formulation containing 0.01% $POCl_3$. Extrudates containing soy protein isolate (SPI) and phosphorylated corn starch with 0.04% $POCl_3$ showcased a marginal increase (0.04%) in expansion ratio (ER), a 0.09% increase in bulk density, a 0.02% increase in oil absorption index (OAI) and a marginal decrease of 0.27% in degree of starch gelatinization (DSG), and a significant increase of 21.5% in water absorption index (WAI) when compared with the extrudate (SPI–NCS) prepared using SPI and NCS. From a commercialization standpoint, the application of phosphorylated starch presents several benefits. Higher bulk density and moderate expansion ratio of the SPI–PCS HMMAs contribute to chewier, more cohesive and firm texture that mimics the mouthfeel of a real animal muscle meat. Moreover, higher water and oil absorption indices of the SPI–PCS HMMAs indicate juicier final product after cooking and improved moisture retention with reduced chances of dryness. PCS serves as an efficient and cost-effective structuring hydrocolloid. It offers a practical alternative to high-purity proteins and commercial hydrocolloids, such as methylcellulose, in plant-based meat substitute formulations. Specifically, PCS has better water-binding ability and gelation compatibility in protein mixtures during high-moisture extrusion. It also supports clean-label formulations, lowers processing heat requirements, and improves the fibrous structure. Additionally, the improved capabilities of PCS create numerous application possibilities across a range of plant-based product types, such as meat substitutes (nuggets, patties, and fillets) and dairy substitutes (cheese alternatives and creamers). Its suitability for various protein matrices and extrusion parameters makes it a flexible and adaptable ingredient for manufacturers looking to innovate in the plant-based industry. In summary, phosphorylated starch, especially PCS obtained with 0.01 and 0.04% $POCl_3$, presents a promising, safe, and practical ingredient that can significantly enhance the quality, cost-effectiveness, and market appeal of plant-based meat substitutes.

# Author contributions

R. Arjun: conceptualization; data curation; formal analysis; investigation; methodology; software; supervision; visualization; roles/writing – original draft; writing – review & editing. R. Keerthi: conceptualization; data curation; formal analysis; investigation; methodology; software; supervision; visualization; roles/writing – original draft; writing – review & editing. P. Monica: software; validation; writing – review & editing. K. V. Ragavan: conceptualization; funding acquisition; project administration; resources; supervision; validation; review & editing.

# Conflicts of interest

There are no conflicts to declare.

# Data availability

The authors declare that experimental data reported in the manuscript are available and can be presented for any clarifications with necessary approvals from the organization.

# Acknowledgements

The authors thank SERB for the startup research grant (SRG/2021/000427). The authors also thank the Director of CSIR NIIST for providing the necessary infrastructure to carry out the work and for encouragement.

# References

1 D. Lam, The Next 2 Billion: Can the World Support 10 Billion People?, *Popul. Dev. Rev*, 2025, **51**, 63–102.
2 H. Górska-Warsewicz, W. Laskowski, O. Kulykovets, A. Kudlińska-Chylak, M. Czeczotko and K. Rejman, Food Products as Sources of Protein and Amino Acids—The Case of Poland, *Nutrients*, 2018, **10**, 1977.
3 M. Henchion, M. Hayes, A. M. Mullen, M. Fenelon and B. Tiwari, Future Protein Supply and Demand: Strategies and Factors Influencing a Sustainable Equilibrium, *Foods*, 2017, **6**, 53.
4 L. Cesoniene, M. Dapkiene and D. Sileikiene, The impact of livestock farming activity on the quality of surface water, *Environ. Sci. Pollut. Res.*, 2019, **26**, 32678–32686.

 

5 N. I. Agudelo Higuita, R. LaRocque and A. McGushin, Climate change, industrial animal agriculture, and the role of physicians – Time to act, *J. Clim. Change Health*, 2023, **13**, 100260.
6 J. Poore and T. Nemecek, Reducing food's environmental impacts through producers and consumers, *Science*, 2018, **360**, 987–992.
7 *Sustainable Protein Sources*, ed. S. R. Nadathur, P. K. J. P. D. Wanasundara and L. Scanlin, 2nd edn, 2023, vol. 1.
8 HSI, Animal agriculture and climate change resources | Humane World for Animals, https://www.humaneworld.org/en/news/animal-agriculture-and-climate-change-resources, accessed 7 June 2025.
9 M. Bruno, M. Thomsen, F. M. Pulselli, N. Patrizi, M. Marini and D. Caro, The carbon footprint of Danish diets, *Clim. Change*, 2019, **156**, 489–507.
10 I. Ismail and N. Huda, in *Future Foods*, ed. R. Bhat, Academic Press, 2022, pp. 351–373.
11 K. Liu, *Soybeans as Functional Foods and Ingredients*, AOCS Publishing, New York, 1st edn., 2004.
12 L. Sha and Y. L. Xiong, Plant protein-based alternatives of reconstructed meat: Science, technology, and challenges, *Trends Food Sci. Technol.*, 2020, **102**, 51–61.
13 K. Kyriakopoulou, J. K. Keppler and A. J. van der Goot, Functionality of Ingredients and Additives in Plant-Based Meat Analogues, *Foods*, 2021, **10**, 600.
14 J. s. Chen, C. m. Lee and C. Crapo, Linear Programming and Response Surface Methodology to Optimize Surimi Gel Texture, *J. Food Sci.*, 1993, **58**, 535–536.
15 J.-Y. Li and A.-I. Yeh, Effects of starch properties on rheological characteristics of starch/meat complexes, *J. Food Eng.*, 2003, **57**, 287–294.
16 S. Samard, B.-Y. Gu and G.-H. Ryu, Effects of extrusion types, screw speed and addition of wheat gluten on physicochemical characteristics and cooking stability of meat analogues, *J. Sci. Food Agric.*, 2019, **99**, 4922–4931.
17 C. Onyango, C. Mutungi, G. Unbehend and M. G. Lindhauer, Rheological and textural properties of sorghum-based formulations modified with variable amounts of native or pregelatinised cassava starch, *LWT–Food Sci. Technol.*, 2011, **44**, 687–693.
18 M. Obadi, Y. Chen, Y. Qi, S. Liu and B. Xu, Effects of different pre-gelatinized starch on the processing quality of high value-added Tartary buckwheat noodles, *Food Measure*, 2020, **14**, 3462–3472.
19 X. He, W. Xia, R. Chen, T. Dai, S. Luo, J. Chen and C. Liu, A new pre-gelatinized starch preparing by gelatinization and spray drying of rice starch with hydrocolloids, *Carbohydr. Polym.*, 2020, **229**, 115485.
20 S. Hedayati, F. Shahidi, A. Koocheki, A. Farahnaky and M. Majzoobi, Physical properties of pregelatinized and granular cold water swelling maize starches at different pH values, *Int. J. Biol. Macromol.*, 2016, **91**, 730–735.
21 B. C. Maniglia, N. Castanha, P. Le-Bail, A. Le-Bail and P. E. D. Augusto, Starch modification through environmentally friendly alternatives: a review, *Crit. Rev. Food Sci. Nutr.*, 2021, **61**, 2482–2505.
22 Z. ud-Din, H. Xiong and P. Fei, Physical and chemical modification of starches: A review, *Crit. Rev. Food Sci. Nutr.*, 2017, **57**, 2691–2705.
23 M. Nikbakht Nasrabadi, A. Sedaghat Doost and R. Mezzenga, Modification approaches of plant-based proteins to improve their techno-functionality and use in food products, *Food Hydrocolloids*, 2021, **118**, 106789.
24 K. Lewicka, P. Siemion and P. Kurcok, Chemical Modifications of Starch: Microwave Effect, *Int. J. Polym. Sci.*, 2015, **2015**, e867697.
25 S. Lim and P. A. Seib, Preparation and Pasting Properties of Wheat and Corn Starch Phosphates, *Cereal Chem.*, 1993, **70**, 137–144.
26 H.-J. Chung, K.-S. Woo and S.-T. Lim, Glass transition and enthalpy relaxtion of cross-linked corn starches, *Carbohydr. Polym.*, 2004, **55**, 9–15.
27 P. Wongphan, C. Nerin and N. Harnkarnsujarit, Modifying Cassava Starch *via* Extrusion with Phosphate, Erythorbate and Nitrite: Phosphorylation, Hydrolysis and Plasticization, *Polymers*, 2024, **16**, 2787.
28 L. Kaur, J. Singh and N. Singh, Effect of cross-linking on some properties of potato (Solanum tuberosum L.) starches, *J. Sci. Food Agric.*, 2006, **86**, 1945–1954.
29 M. F. Ramadan and M. Z. Sitohy, Phosphorylated Starches: Preparation, Properties, Functionality, and Techno-Applications, *Starch - Stärke*, 2020, **72**, 1900302.
30 J. Zhang, A. Li and A. Wang, Study on superabsorbent composite. VI. Preparation, characterization and swelling behaviors of starch phosphate-graft-acrylamide/attapulgite superabsorbent composite, *Carbohydr. Polym.*, 2006, **65**, 150–158.
31 A. Blennow, T. H. Nielsen, L. Baunsgaard, R. Mikkelsen and S. B. Engelsen, Starch phosphorylation: a new front line in starch research, *Trends Plant Sci.*, 2002, **7**, 445–450.
32 Y. Thakur, R. Thory, K. S. Sandhu, M. Kaur, A. Sinhmar and A. K. Pathera, Effect of selected physical and chemical modifications on physicochemical, pasting, and morphological properties of underutilized starch from rice bean (Vigna umbellata), *J Food Sci Technol*, 2021, **58**, 4785–4794.
33 S. Mehboob, T. M. Ali, F. Alam and A. Hasnain, Dual modification of native white sorghum (Sorghum *bicolor*) starch *via* acid hydrolysis and succinylation, *LWT–Food Sci. Technol.*, 2015, **64**, 459–467.
34 J. J. E. Al. Jagruti Jankar, *et al.*, TJPRC, Evaluation of Physicochemical Properties of Guar Gum- Antioxidants Emulsion Coatings, *IJMPERD*, 2020, **10**, 6985–6992.
35 A. A. Ibikunle, N. O. Sanyaolu, S. T. Yussuf, A. L. Ogunneye, O. A. Badejo and O. M. Olaniyi, Effects of chemical modification on functional and physical properties of African star apple kernel (Chrysophyllum albidnum) starch, *Afr. J. Pure Appl. Chem.*, 2019, **13**, 1–11.
36 Y. Su, J. Guan, S. Liu, Y. Zhu, L. Hu, Y. Zhang, F. Lu and M. Zhu, Effects of Cassava and Modified Starch on the Structural and Functional Characteristics of Peanut Protein-Based Meat Analogs, *Foods*, 2025, **14**, 2849.

37 Nutrition Division, *Compendium of Food Additive Specifications*, FAO/WHO, ROME, 1st edn, 2014.
38 United States, *US Pat. US2754232A*, 1956.
39 A. Rahim, G. Hutomo and Jusman, Effect Of Phosphorylation On The Physical And Chemical Characteristics Of Arenga Starch, *Int. J. Biol., Pharm. Allied Sci.*, 2013, **2**(11), 1973–1985.
40 S. Zhou and G. Huang, Preparation, structure and activity of polysaccharide phosphate esters, *Biomed. Pharmacother.*, 2021, **144**, 112332.
41 X. Kong, D. Qiu, X. Ye, J. Bao, Z. Sui, J. Fan and W. Xiang, Physicochemical and crystalline properties of heat-moisture-treated rice starch: combined effects of moisture and duration of heating, *J. Sci. Food Agric.*, 2015, **95**, 2874–2879.
42 G. A. Mountain and C. D. Keating, in *Methods in Enzymology*, ed. C. D. Keating, Academic Press, 2021, vol. 646, pp. 115–142.
43 K. E. Ileleji, A. A. Garcia, A. R. P. Kingsly and C. L. Clementson, Comparison of Standard Moisture Loss-on-Drying Methods for the Determination of Moisture Content of Corn Distillers Dried Grains with Solubles, *J. AOAC Int.*, 2010, **93**, 825–832.
44 A. B. Mortensen and H. Wallin, Gravimetric Determination of Ash in Foods: NMKL Collaborative Study, *J. Assoc. Off. Anal. Chem.*, 1989, **72**, 481–483.
45 S. S. Nielsen, *Food Analysis*, Springer New York, NY, Boston, MA, 4th edn., 2010.
46 N. J. Thiex, H. Manson, S. Anderson, J.-Å. Persson, Collaborators:, S. Anderson, E. Bogren, G. Bolek, D. Budde, C. Ellis, S. Eriksson, G. Field, E. Frankenius, C. Henderson, C. Henry, M. Kapphahn, L. Lundberg, H. Manson, J. Moller, M. Russell, J. Sefert-Schwind and M. Spann, Determination of Crude Protein in Animal Feed, Forage, Grain, and Oilseeds by Using Block Digestion with a Copper Catalyst and Steam Distillation into Boric Acid: Collaborative Study, *J. AOAC Int.*, 2002, **85**, 309–317.
47 N. J. Thiex, S. Anderson, B. Gildemeister, W. Adcock, J. Boedigheimer, E. Bogren, R. Coffin, K. Conway, A. DeBaker, E. Frankenius, M. Gramse, P. Hogan, T. Knese, J. MacDonald, J. Muller, R. Royle, M. Russell, F. Shafiee, B. Shreve, J. Sieh, M. Spann, E. Töpler and M. Watts, Crude Fat, Hexanes Extraction, in Feed, Cereal Grain, and Forage (Randall/Soxtec/Submersion Method): Collaborative Study, *J. AOAC Int.*, 2003, **86**, 899–908.
48 N. J. E. de Mesa, S. Alavi, N. Singh, Y.-C. Shi, H. Dogan and Y. Sang, Soy protein-fortified expanded extrudates: Baseline study using normal corn starch, *J. Food Eng.*, 2009, **90**, 262–270.
49 H. Liu, R. L. Hebb, N. Putri and S. S. H. Rizvi, Physical properties of supercritical fluid extrusion products composed of milk protein concentrate with carbohydrates, *Int. J. Food Sci. Technol.*, 2017, **53**(3), 847–856, DOI: 10.1111/ijfs.13624.
50 I. Zahari, F. Ferawati, J. K. Purhagen, M. Rayner, C. Ahlström, A. Helstad and K. Östbring, Development and Characterization of Extrudates Based on Rapeseed and Pea Protein Blends Using High-Moisture Extrusion Cooking, *Foods*, 2021, **10**, 2397.
51 G. G. Birch and R. J. Priestley, Degree of Gelatinisation of Cooked Rice, *Starch - Stärke*, 1973, **25**, 98–100.
52 A. M. Stephen and G. O. Phillips, *Food Polysaccharides and Their Applications*, CRC Press, Boca Raton, 2nd edn., 2016.
53 N. Shah, R. K. Mewada and T. Mehta, Crosslinking of starch and its effect on viscosity behaviour, *Rev. Chem. Eng.*, 2016, **32**, 265–270.
54 R. J. Delley, A. C. O'Donoghue and D. R. W. Hodgson, Hydrolysis Studies of Phosphodichloridate and Thiophosphodichloridate Ions, *J. Org. Chem.*, 2012, **77**, 5829–5831.
55 S. W. Cui, *Food Carbohydrates Chemistry, Physical Properties, and Applications*, CRC Press, Boca Raton, 1st edn., 2005.
56 H. Singh, J.-H. Lin, W.-H. Huang and Y.-H. Chang, Influence of amylopectin structure on rheological and retrogradation properties of waxy rice starches, *J. Cereal Sci.*, 2012, **56**, 367–373.
57 EFSA Panel on Food Additives and Nutrient Sources added to Food (ANS), A. Mortensen, F. Aguilar, R. Crebelli, A. Di Domenico, B. Dusemund, M. J. Frutos, P. Galtier, D. Gott, U. Gundert-Remy, C. Lambré, J.-C. Leblanc, O. Lindtner, P. Moldeus, P. Mosesso, D. Parent-Massin, A. Oskarsson, I. Stankovic, I. Waalkens-Berendsen, M. Wright, M. Younes, P. Tobback, Z. Horvath, S. Tasiopoulou and R. A. Woutersen, Re-evaluation of oxidised starch (E 1404), monostarch phosphate (E 1410), distarch phosphate (E 1412), phosphated distarch phosphate (E 1413), acetylated distarch phosphate (E 1414), acetylated starch (E 1420), acetylated distarch adipate (E 1422), hydroxypropyl starch (E 1440), hydroxypropyl distarch phosphate (E 1442), starch sodium octenyl succinate (E 1450), acetylated oxidised starch (E 1451) and starch aluminium octenyl succinate (E 1452) as food additives, *EFSA J.*, 2017, **15**, e04911.
58 F. J. Polnaya, Haryadi, D. W. Marseno and M. N. Cahyanto, Preparation and Properties of Phosphorylated Sago Starches, *Sago Palm*, 2012, **20**, 3–11.
59 S. Lim and P. Seib, Location of phosphate esters in a wheat starch phosphate by 31P-nuclear magnetic resonance spectroscopy, *Cereal Chem.*, 1993, **70**, 145–152.
60 M. Wootton and Haryadi, Effects of starch type and preparation conditions on substituent distribution in hydroxypropyl starches, *J. Cereal Sci.*, 1992, **15**, 181–184.
61 F. J. Plolnaya, D. W. Marseno and M. N. Cahyanto, Effects of phosphorylation and cross-linking on the pasting properties and molecular structure of sago starch, *Int. Food Res. J.*, 2013, **20**, 1609–1615.
62 E. H. Nabeshima and M. V. E. Grossmann, Functional properties of pregelatinized and cross-linked cassava starch obtained by extrusion with sodium trimetaphosphate, *Carbohydr. Polym.*, 2001, **45**, 347–353.
63 J. Singh, L. Kaur and O. J. McCarthy, Factors influencing the physico-chemical, morphological, thermal and rheological properties of some chemically modified starches for food applications—A review, *Food Hydrocolloids*, 2007, **21**, 1–22.

 

64 L. Mirmoghtadaie, M. Kadivar and M. Shahedi, Effects of cross-linking and acetylation on oat starch properties, *Food Chem.*, 2009, **116**, 709–713.
65 S. Fukuzawa, T. Ogawa, K. Nakagawa and S. Adachi, Kinetics on the turbidity change of wheat starch during its retrogradation, *Biosci., Biotechnol., Biochem.*, 2016, **80**, 1609–1614.
66 L. Yang, Y. Zhou, Y. Wu, X. Meng, Y. Jiang, H. Zhang and H. Wang, Preparation and physicochemical properties of three types of modified glutinous rice starches, *Carbohydr. Polym.*, 2016, **137**, 305–313.
67 Y. Zheng, L. Hu, N. Ding, P. Liu, C. Yao and H. Zhang, Physicochemical and structural characteristics of the octenyl succinic ester of ginkgo starch, *Int. J. Biol. Macromol.*, 2017, **94**, 566–570.
68 J. Rożnowski, L. Juszczak, B. Szwaja and I. Przetaczek-Rożnowska, Effect of Esterification Conditions on the Physicochemical Properties of Phosphorylated Potato Starch, *Polymers*, 2021, **13**, 2548.
69 H. Liu, L. Ramsden and H. Corke, Physical Properties and Enzymatic Digestibility of Phosphorylated ae, wx, and Normal Maize Starch Prepared at Different pH Levels, *Cereal Chem.*, 1999, **76**, 938–943.
70 N. Hu, L. Li, E. Tang and X. Liu, Structural, physicochemical, textural, and thermal properties of phosphorylated chestnut starches with different degrees of substitution, *J. Food Process. Preserv.*, 2020, **44**, e14457.
71 R. Sindhu and B. S. Khatkar, Thermal, structural and textural properties of amaranth and buckwheat starches, *J Food Sci Technol*, 2018, **55**, 5153–5160.
72 C. Liu, H. Yan, S. Liu and X. Chang, Influence of Phosphorylation and Acetylation on Structural, Physicochemical and Functional Properties of Chestnut Starch, *Polymers*, 2022, **14**, 172.
73 C. Cao, D. Wei, F. Xuan, C. Deng, J. Hu and Y. Zhou, Comparative study on the structure and physicochemical of waxy rice starch by phosphorylation, lactylation and dual-modified, *Food Sci. Technol.*, 2022, **42**, e18622.
74 H. Dong and T. Vasanthan, Effect of phosphorylation techniques on structural, thermal, and pasting properties of pulse starches in comparison with corn starch, *Food Hydrocolloids*, 2020, **109**, 106078.
75 H. Marta, Y. Cahyana, S. Bintang, G. P. Soeherman and M. Djali, Physicochemical and pasting properties of corn starch as affected by hydrothermal modification by various methods, *Int. J. Food Prop.*, 2022, **25**, 792–812.
76 N. A. Landerito and Y.-J. Wang, Preparation and Properties of Starch Phosphates Using Waxy, Common, and High-Amylose Corn Starches. I. Oven-Heating Method, *Cereal Chem.*, 2005, **82**, 264–270.
77 P. Bhatt, V. Kumar, H. Rastogi, M. K. Malik, R. Dixit, S. Garg, G. Kapoor and S. Singh, Functional and Tableting Properties of Alkali-Isolated and Phosphorylated Barnyard Millet (Echinochloa esculenta) Starch, *ACS Omega*, 2023, **8**, 30294–30305.
78 L. Wei, Z. Zhengqiao, W. Jie, X. Zhenzhen and L. Zhi, *Phosphorylation/caproylation of Cornstarch to Improve its Adhesion to PLA and Cotton Fibers*, RSC, 2010, DOI: 10.1039/c9ra07384a.
79 E. Schmid, A. Farahnaky, B. Adhikari and P. J. Torley, High moisture extrusion cooking of meat analogs: A review of mechanisms of protein texturization, *Compr. Rev. Food Sci. Food Saf.*, 2022, **21**, 4573–4609.
80 S. Mishal, S. Kanchan, P. Bhushette and S. K. Sonawane, in *Food Science and Applied Biotechnology*, FSAB, 1st edn., 2022, vol. 5.
81 B. Gu, M. D. P. Masli and G. M. Ganjyal, Whole faba bean flour exhibits unique expansion characteristics relative to the whole flours of lima, pinto, and red kidney beans during extrusion, *J. Food Sci.*, 2020, **85**, 404–413.
82 J.-S. Lee, I. Choi and J. Han, Construction of rice protein-based meat analogues by extruding process: Effect of substitution of soy protein with rice protein on dynamic energy, appearance, physicochemical, and textural properties of meat analogues, *Food Res. Int.*, 2022, **161**, 111840.
83 S. Q. Li, H. Q. Zhang, Z. T. Jin and F. H. Hsieh, Textural modification of soya bean/corn extrudates as affected by moisture content, screw speed and soya bean concentration, *Int. J. Food Sci. Technol.*, 2005, **40**, 731–741, DOI: 10.1111/j.1365-2621.2005.00993.x.
84 A. Arhaliass, J. Legrand, P. Vauchel, F. Fodil-Pacha, T. Lamer and J. M. Bouvier, The effect of wheat and maize flours properties on the expansion mechanism during extrusion cooking, *Food Bioprocess Technol.*, 2009, **2**, 186–193.
85 S. Ilo, U. Tomschik, E. Berghofer and N. Mundigler, The Effect of Extrusion Operating Conditions on the Apparent Viscosity and the Properties of Extrudates in Twin-Screw Extrusion Cooking of Maize Grits, *LWT–Food Sci. Technol.*, 1996, **29**, 593–598.
86 M. A. Brennan, J. A. Monro and C. S. Brennan, Effect of inclusion of soluble and insoluble fibres into extruded breakfast cereal products made with reverse screw configuration, *Int J of Food Sci Tech*, 2008, **43**, 2278–2288.
87 S. Hong, Y. Shen and Y. Li, Physicochemical and Functional Properties of Texturized Vegetable Proteins and Cooked Patty Textures: Comprehensive Characterization and Correlation Analysis, *Foods*, 2022, **11**, 2619.
88 S. I. Fletcher, P. Richmond and A. C. Smith, An experimental study of twin screw extrusion cooking of maize grits, *J. Food Eng.*, 1985, **4**, 291–312.
89 S. Ilo, Y. Liu and E. Berghofer, Extrusion Cooking of Rice Flour and Amaranth Blends, *LWT–Food Sci. Technol.*, 1999, **32**, 79–88.
90 C. Barron, B. Bouchet, G. Della Valle, D. J. Gallant and V. Planchot, Microscopical Study of the Destructuring of Waxy Maize and Smooth Pea Starches by Shear and Heat at Low Hydration, *J. Cereal Sci.*, 2001, **33**, 289–300, DOI: 10.1006/jcrs.2000.0368.
91 A. Altan, K. L. McCarthy and M. Maskan, Evaluation of snack foods from barley–tomato pomace blends by extrusion processing, *J. Food Eng.*, 2008, **84**, 231–242.
92 R. Alonso, E. Orúe, M. J. Zabalza, G. Grant and F. Marzo, Effect of extrusion cooking on structure and functional

properties of pea and kidney bean proteins, *J. Sci. Food Agric.*, 2000, **80**, 397–403.

93 T. Y. Liu, Y. Ma, S. F. Yu, J. Shi and S. Xue, The effect of ball milling treatment on structure and porosity of maize starch granule, *Innovative Food Sci. Emerging Technol.*, 2011, **12**, 586–593.

94 N. Yousf, F. Nazir, R. Salim, H. Ahsan and A. Sirwal, Water solubility index and water absorption index of extruded product from rice and carrot blend, *J. Pharmacogn. Phytochem.*, 2017, **6**(6), 2165–2168.

95 C. Omohimi, S. Philip, K. O. Sarafadeen and L. Sanni, Effect of Thermo-extrusion Process Parameters on Selected Quality Attributes of Meat Analogue from Mucuna Bean Seed Flour, *Niger. Food J.*, 2014, **32**, 21–30.

96 M. E. Camire, A. Camire and K. Krumhar, Chemical and nutritional changes in foods during extrusion, *Crit. Rev. Food Sci. Nutr.*, 1990, **29**, 35–57.

97 X. Yan, D. J. McClements, S. Luo, C. Liu and J. Ye, Recent advances in the impact of gelatinization degree on starch: Structure, properties and applications, *Carbohydr. Polym.*, 2024, **340**, 122273.

98 X. Wang, S. Liu and Y. Ai, Gelation mechanisms of granular and non-granular starches with variations in molecular structures, *Food Hydrocolloids*, 2022, **129**, 107658.

99 M. Du, T. Cao, M. Yu, C. Zhang and W. Xu, Effect of heat-moisture treatment on physicochemical properties of chickpea starch, *Food Sci. Technol.*, 2023, **43**, e108822.